AJP

ISSN : 0971 - 3093

Vol 33, No 12, December 2024

ASIAN JOURNAL OF PHYSICS

An International Peer Reviewed Research Journal

Special issue in honour of Dr Daniel Malacara-Hernández

Dr Daniel Malacara-Hernández

Guest Editors: Amalia Martínez-García & Daniel Malacara-Doblado

ANITA PUBLICATIONS
FF-43, 1st Floor, Mangal Bazar, Laxmi Nagar, Delhi-110 092, India
B O : 2, Pasha Court, Williamsville, New York-14221-1776, USA

Asian Journal of Physics
Vol. 33, No 12 (2024) 793-802
Available on: www.asianjournalofphysics.com

Investigation of photoactive properties in $LiMn_2O_4$ cathode for lithium-ion batteries

D A Medina-Sanchez[1], J S Martinez-Flores[1], S Rodriguez-Carrera[1], L S Valle-Garcia[1],
C D Mena-Muñoz[1], L Skokan[2], S Obernberger[2], A Ruediger[2], R Garza-Hernandez[1], F Morales-Morales[1],
A Benitez-Lara[3], and F Ambriz-Vargas[1]

*[1]Centro de Investigaciones en Óptica, A. C., Loma del Bosque 115, Lomas del Campestre,
León, Gto, México. C.P. 37150*

[2]Centre Énergie, Matériaux et Télécommunications, INRS, 1650 Lionel-Boulet, Varennes, Québec, J3X1S2, Canada.

*[3] Instituto Nacional de Astrofísica, Óptica y Electrónica, Luis Enrique Erro 1,
Sta María Tonanzintla, 72840 San Andrés Cholula, Puebla*

Dedicated to Prof (Dr) Daniel Malacara-Hernández

In the current era of energy transition, one of the main challenges in introducing electric vehicles to the market is the long charging times compared to gasoline refueling. This communication evaluates the photoactive processes in cathode electrode used in lithium-ion batteries. This research presents the fabrication of a CR 2032-coin cell battery equipped with a transparent quartz window, allowing for monitoring of the electrochemical properties of lithium-ion batteries in response to light exposure. The novelty of this research lies in the experimental demonstration of the photoactive process of $LiMn_2O_4$ cathodes when exposed to low-power UV light (4W). Specifically, it was shown that under UV light irradiation, the photoactivity of the $LiMn_2O_4$ material generates electron-hole pairs, resulting in reduced electronic resistance at the electrode/electrolyte interface. This reduction in resistance ultimately leads to shorter charging times.

doi: 10.54955.AJP.33.12.2024.793-802

Keywords: Lithium-ion battery; Photoactive properties; $LiMn_2O_4$ cathode; Energy transition.

---

1 Introduction

The 2050 challenge, proposed by the International Renewable Energy Agency (IRENA), aims to achieve global carbon neutrality by mid-century. To achieve this goal, energy storage devices such as lithium-ion batteries (Li-ion) are crucial for the energy transition. This technology plays a vital role in two sectors: (1) In the renewable energy sector, one of the challenges of wind and solar energy is their intermittent nature (they generate electricity only when the sun is shining or the wind is blowing). In such a scenario, lithium-ion batteries can store renewable energy during peak generation periods and can be used when generation is low. (2) In the transport sector, lithium-ion batteries stand out as the key technology for the electrification of transport because: (1) Their high gravimetric energy density (200 – 250 Wh/kg), (2) Rechargeable nature (2000 – 3000 charge/discharge cycles), and (3) The potential for lower greenhouse gas emissions make lithium-ion batteries an attractive technology for achieving sustainable transportation [1].

Corresponding author
e mail: fambriz@cio.mx (F Ambriz-Vargas)

Lithium-ion batteries with $LiMn_2O_4$-based cathodes are essential for advancing the electrification of the automobile industry. The layered structure of this cathode oxide material enables efficient lithium-ion intercalation and deintercalation, resulting in a high capacity of 200–250 Wh/kg [4]. This high capacity allows electric vehicles to travel 300-400 km on a single charge. Moreover, these batteries demonstrate thermal stability, a crucial feature for preventing overheating and potential battery fires [5]. Recent advancements have shown that a dry fabrication process, utilizing a physical vapor deposition technique called sputtering, can effectively produce $LiMn_2O_4$ cathode materials. This method achieves a specific capacity of 119 mAh/g, making it a promising option for sustainable battery fabrication [6].

One of the challenges in the widespread adoption of electric vehicles is the time it takes to charge them [7]. The electric vehicle industry aims to achieve charging times of 15 to 40 minutes to charge from 20% to 80% State of Charge (SoC). This goal has the promise to be closer to the refueling time of gasoline vehicles, which typically takes 5-10 minutes [7]. A key issue in fast-charging lithium-ion batteries is the slow ion transport of lithium, which leads to slow ionic diffusion ($D^0_{Li^+} = 10^{-11}$ cm^2/s) [8]. One potential solution to this challenge is to develop a high-conductivity electrolyte medium that minimizes ionic resistance, allowing for faster lithium diffusion inside the electrolyte and at the electrode/electrolyte interface [9,10]. Another potential lies in the photocatalytic properties of the internal battery materials. This approach is based on the interaction between light and materials, specifically utilizing photoactive substances that can enhance the kinetics of lithium-ion transport when exposed to light. In this context, the present research aims to investigate the $LiMn_2O_4$ cathode as a photoactive material within lithium-ion batteries to reduce charging time.

2 Experimental methodology

Sample preparation: In this study to deposit $LiMn_2O_4$, three different substrates were employed, each selected according to the specific characterization technique: stainless steel for electrochemical measurements, silicon for structural analysis, and glass for band gap determination.

The deposition of $LiMn_2O_4$ cathode material was conducted using an on-axis RF magnetron sputtering. The sputtering system utilized in this study was an ATC-Orion deposition system (AJA Sputtering System, Massachusetts, USA). Before deposition, the chamber was evacuated to a base pressure of 10^{-6} Torr. Argon gas served as the sputtering medium (flow of 32 sccm), and the distance between the polycrystalline $LiMn_2O_4$ ceramic disk (American elements, LIMN-OX-02, Purity: 99%, 5.08 cm in diameter and 0.317 cm in thickness) and the substrate was maintained 10 cm. To facilitate the growth of $LiMn_2O_4$ cathode thin films with uniform thickness, the substrate was rotated at a speed of 55 rpm.

The ignition of the argon plasma was initiated at a power of 30 W and a chamber pressure of 30 mTorr. During this initial phase, a shutter was kept in place over the substrate to allow for pre-sputtering of the target surface for 2 minutes. Following this pre-sputtering process, deposition proceeded at an RF power of 150 W and a chamber pressure of 10 mTorr. This occurred in two separate sessions: one hour for thickness measurement and three hours for battery application. The as-deposited films underwent thermal annealing (tube furnace, Thermo Scientific STF55666COMC-1, Lindberg/Blue M) at 500 °C for 1 hour to promote the crystallization of the $LiMn_2O_4$ phase.

Microstructural and structural characterization:

The thickness of the thermally treated samples was examined using a Field Emission Scanning Electron Microscope (JSM-7800F, JEOL, Japan). The surface of the coating was analyzed using Atomic Force Microscopy (Smart SPM1000-AIST-NT Inc.) in tapping mode. The phase formation of the thermally treated coatings was monitored using a Raman spectrometer (Horiba, USA). These measurements were conducted at room temperature with a confocal microscope featuring a 50x objective magnification (NA = 0.5) and a focal spot diameter of 1.2 µm. A laser wavelength of 473 nm was produced by a linearly polarized Cobolt Blues 25 mW diode-pumped solid-state laser (DPSS). In addition, X-ray diffraction analysis was performed using the Bruker D2 phase diffractometer.

CR 2032 Coin cell assembly process:

A coin cell featuring a transparent quartz window (diameter = 3 mm) at the center of the positive casing (Fig 1(a)) was used. The cell was assembled within an argon-filled glove box (LG1200/750TS, Vigor Tech-USA), which maintained H_2O and O_2 levels at approximately 2 ppm.

The components used in the cell assembly included a negative casing, a stainless steel (SS) spacer, a lithium foil counter electrode (diameter = 14 mm), a polypropylene microporous film separator (diameter = 16 mm), a 25 µl drop of 1 mol/L $LiPF_6$ electrolyte, a sputtered film working electrode (diameter = 14 mm), another stainless steel spacer, a stainless steel spring, and a positive casing featuring a transparent quartz window (diameter = 3 mm). After assembly, the coin cells were sealed using a hydraulic crimper (TOB-Df-160, Tob Machine).

Photoinduced battery evaluation:

A custom-made chamber was used to evaluate the photoactive properties of $LiMn_2O_4$, as shown in Fig 1(b). The design of the chamber consists of a sealed black box that blocks ambient light. Inside, there is a UV lamp positioned to emit 254 nm irradiation at a power of 4W. A coin-cell battery with a transparent quartz window is located inside a battery holder within the chamber. The distance between the UV lamp and the battery holder was set at 7 cm. The photoactive properties of the cathode film were evaluated using a potentiostat/galvanostat (VSP-300, Bio Logic-France) equipped with a four-point coin cell holder connection (CCH-8, Bio Logic-France). Galvanostatic charge-discharge tests were conducted within a fixed voltage range of 3.0 to 4.4 V vs. Li/Li^+. Additionally, electrochemical impedance spectroscopy measurements of the cells were performed with an amplitude of 10 mV, covering frequencies from 0.1 Hz to 1 MHz.

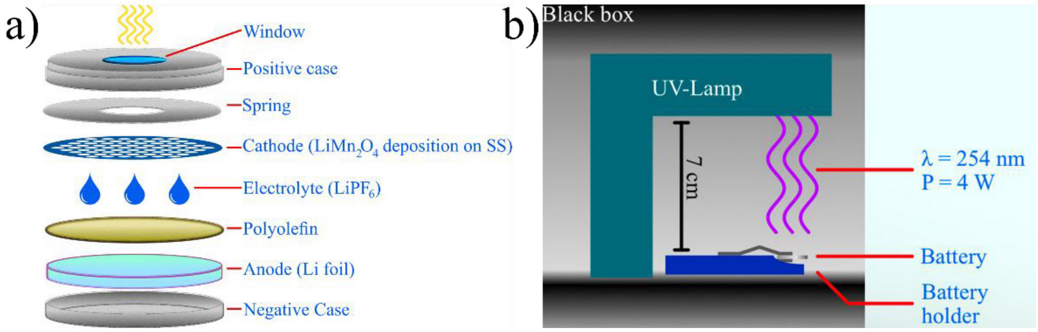

Fig 1. Schematic representation of (a) a coin-cell battery CR2032 with a transparent quartz window and (b) the chamber used to evaluate photoactive properties. SS stands for stainless steel spacer.

3 Results and discussion

Following the thermal treatment, it was conducted an analysis of the microstructural properties of the cathode material. The cross-section of the $LiMn_2O_4$ sample, illustrated in Fig 2(a), exhibits a uniform coating thickness of 47 nm, free of porosity, after one hour of sputtering deposition. The parameters of the sputtering deposition (described in the experimental section) indicate a rate of 0.8 nm per minute, which corresponds to the growth of one uniform monolayer of $LiMn_2O_4$ cubic cell each minute (with dimensions of a = b = c = 8.21 Å). Achieving a uniform thickness is vital for ensuring consistent current distribution across the cathode [11]. Furthermore, the low porosity contributes to enhanced electrical pathways and reduced internal electrical resistance [12]. An atomic force microscope analysis of the surface area of $LiMn_2O_4$ revealed a polycrystalline growth pattern of the film, along with a flat surface roughness (root mean square roughness of 1.2 nm). This smooth surface is beneficial for improved electrolyte wettability and enhanced lithium-ion diffusion [13].

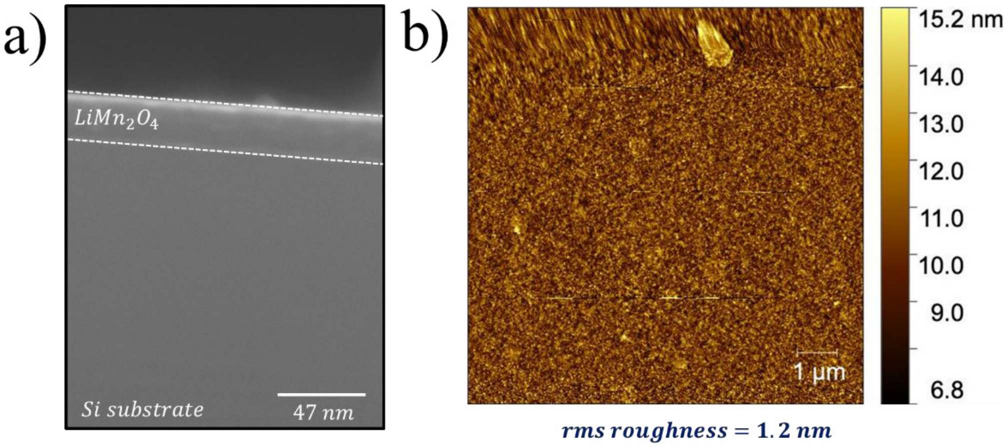

Fig 2. FE-SEM image showing the cross-section of $LiMn_2O_4$ cathode material and (b) Tapping-AFM image of the surface of $LiMn_2O_4$.

The as-sputtered $LiMn_2O_4$ films underwent a thermal treatment at 500°C for one hour to facilitate crystallization. The structural properties of the films were examined using X-ray diffraction and Raman spectroscopy. Figure 3 displays the X-ray diffractogram obtained from the stainless steel substrate along with the $LiMn_2O_4$ cathode film.

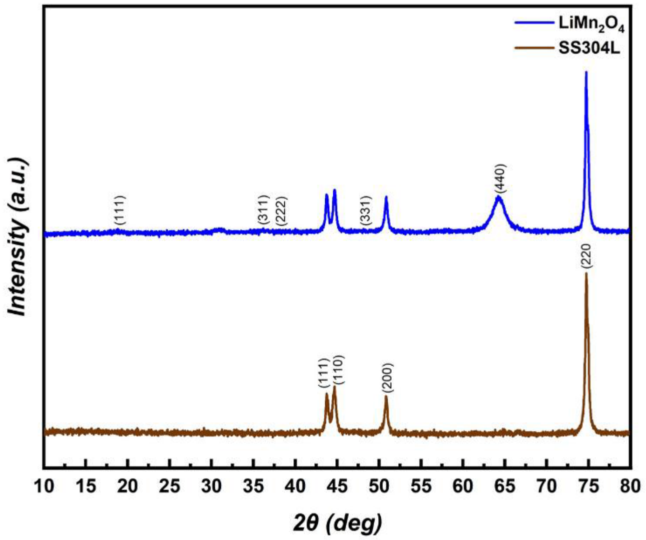

Fig 3. X-ray diffractogram obtained from a stainless steel substrate and a thermally treated $LiMn_2O_4$ coating.

The high-intensity diffraction peaks at 44°, 45°, 51°, and 75° correspond to the stainless steel substrate, while the lower-intensity peaks at 19°, 36°, 37°, 48°, and 65° are associated with the thermally treated coating. These diffraction planes were indexed to the cubic spinel $LiMn_2O_4$ structure (a = b = c =

8.21 Å) with the space group $F\bar{d}3m$ [14]. Due to the smaller volume of the coating in comparison to the substrate, the diffraction peaks of the coating appeared with lower intensity.

To validate the crystallization of the sputtered coatings, additional analysis was conducted using Raman spectroscopy. According to group theory, the cubic spinel $LiMn_2O_4$ structure consists of 14 optical phonon modes (Eq 1).

$$\Gamma_{vib} = A_{1g} + E_g + 3T_{2g} + 4T_{1u} + 2A_{2u} + 2E_u + T_{2u} \tag{1}$$

In this representation, A_{1g}, E_g, and T_{2g} are Raman-active modes, while T_{1u} is an infrared (IR)-active mode. The modes A_{2u}, E_u and T_{2u} are silent, meaning they are neither Raman nor IR-active [15,16]. The expression can be simplified to five Raman modes, though typically only a subset of these modes is observable at room temperature.

The Raman spectra of the $LiMn_2O_4$ cathode coating (Fig 4) exhibit peaks at 360, 480, and 617 cm^{-1}. According to the literature, these active Raman modes correspond to the $LiMn_2O_4$ spinel phase. Specifically, the peak at 360 cm^{-1} is related to the bending vibrations of the MnO_6 octahedra, the peak at 480 cm^{-1} corresponds to the asymmetric stretching of Mn–O bond, and the peak at 617 cm^{-1} is associated with the symmetric stretching vibrations of Mn–O bond within the MnO_6 octahedra, which is the most prominent peak in $LiMn_2O_4$ [16]. Based on the findings of Raman spectroscopy and X-ray diffraction analyses, the formation of the cubic spinel $LiMn_2O_4$ structure in the thermally treated samples was confirmed.

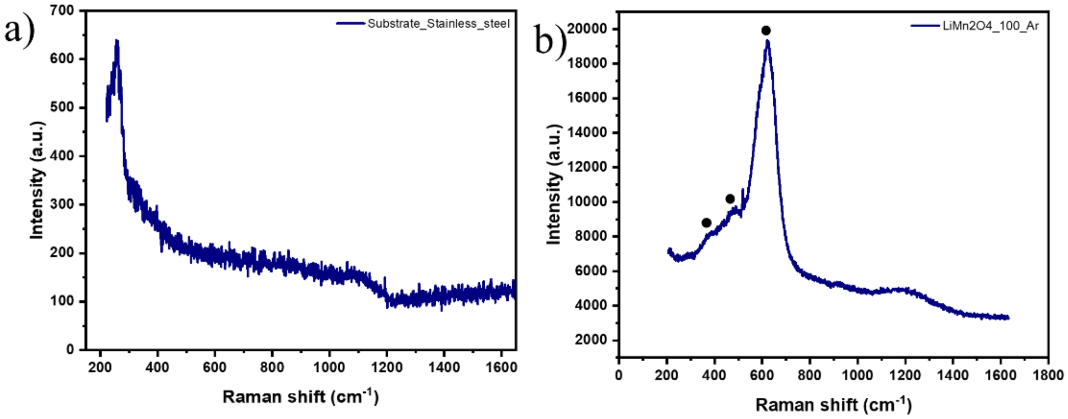

Fig 4. Raman spectrum obtained from (a) A stainless steel substrate and (b) A thermally treated $LiMn_2O_4$ coating.

The results of the UV-VIS absorption spectroscopy measurements are presented in Fig 5. The band gap is found to be 2.71 eV, which places the $LiMn_2O_4$ cathode material within the UV region of the electromagnetic spectrum, corresponding to wavelengths around 458 nm [17]. Typically, an ideal photoactive material for UV-VIS activity has a band gap between 1.8 and 3.2 eV, allowing absorption across a broader spectrum [18]. The calculated band gap of 2.71 eV indicates that $LiMn_2O_4$ can effectively absorbs ultraviolet light, providing sufficient energy to excite electrons from the valence band to the conduction band, thus creating electron-hole pairs [17-19]. In this context, the chamber designed to evaluate the photoactivity of the $LiMn_2O_4$ cathode material is equipped with a UV-VIS lamp (254 nm) powered by a small 4W source (Fig 1(b)).

In the evaluation of the photoactive process, a $LiMn_2O_4$ thin film material was assembled as a cathode inside a CR 2032 lithium coin cell battery, which featured a transparent crystal quartz window (Fig 1(a)). The purpose of the window is to enable the interaction of the $LiMn_2O_4$ surface with UV light radiation. This evaluation process also involved using a box with black inner walls to block ambient light, as well as a potentiostat/galvanostat system to run charge/discharge curves both with and without UV-VIS radiation.

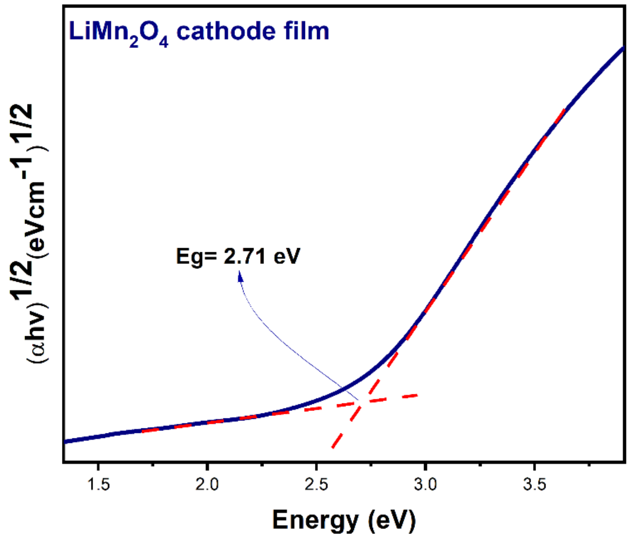

Fig 5. Direct band energy diagram of the $LiMn_2O_4$ thin film.

The battery was cycled between 3.0 and 4.3 V vs. Li/Li^+ at a fixed current of 5 microamperes. The obtained charge/discharge curves with the light switched OFF and ON are presented in Fig 6. Generally, both curves resemble with the typical shape of $LiMn_2O_4$ curves reported in the literature [20,21].

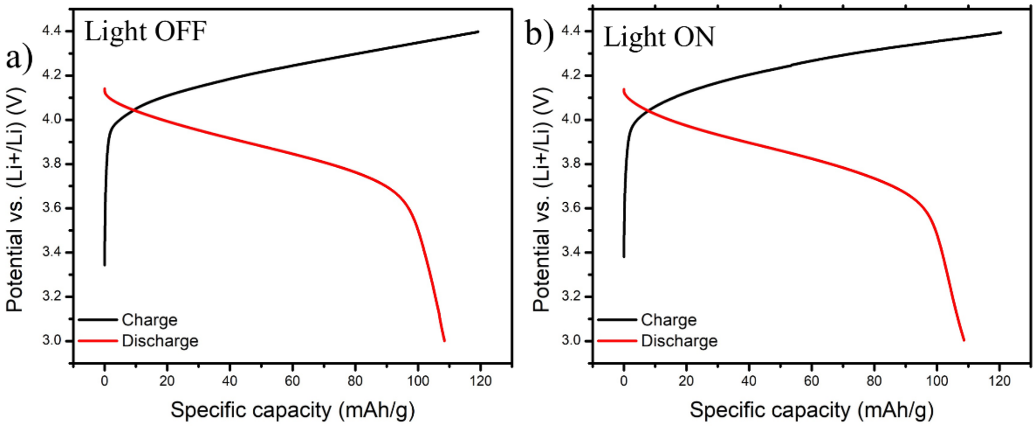

Fig 6. A comparison of a CR2032 coin cell battery (a) without UV light irradiation and (b) with UV light irradiation.

To quantify the discharge capacity, several parameters were considered, including the cathode area (140.975 mm^2 for the stainless steel mesh), cathode thickness (180 nm from three hours of sputtering deposition), and the density of $LiMn_2O_4$ (4.58 g/cm^3). As shown in Fig 6, the CR 2032-coin cell battery with $LiMn_2O_4$ exhibited a discharge capacity of 115 mAh/g in dark conditions and 116 mAh/g under UV-VIS irradiation. These discharge capacities are comparable to the theoretical capacity of spinel $LiMn_2O_4$(148 mAh/g) and to experimental values reported in the literature (124 mAh/g) [20,21].

The exposure to UV light does not significantly affect the discharge capacity of the battery. However, another method to assess the impact of the photoinduced process is by analyzing the charging curve over time (see Fig 7). This type of plot enables us to quantify the charging time. As shown in Fig 7, the time taken to charge from 3.3 V to 4.2 V under dark conditions is 54.8 minutes (or 3,293 seconds). In contrast, under UV light irradiation, the charging time is reduced to 49.8 minutes (or 2,989 seconds), indicating a time savings of nearly 4 minutes. Due to the risk of battery heating and lithium plating when charging to a 100% state of charge, it is preferred to evaluate the charging duration at a voltage lower than its maximum (4.4V) [23].

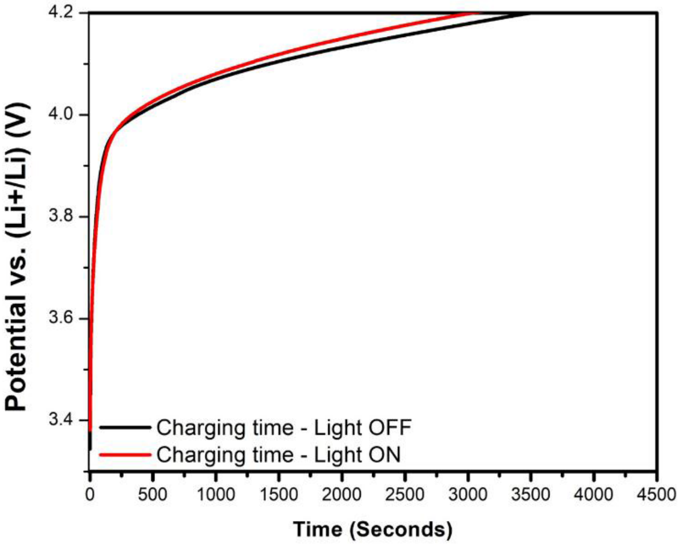

Fig 7. Comparison of the charging time of a CR2032 coin cell battery without UV light irradiation and with UV light irradiation.

While this small reduction in time (4 minutes) may be attributed to the relatively low power of the UV light lamp (4 Watts), it could also suggest improved lithium-ion diffusion at the electrode-electrolyte interface, thereby shortening the intercalation time of lithium ions during charging. To validate this hypothesis, electrochemical impedance spectroscopy was performed on the CR 2032-coin cell battery.

Figure 8(a) shows the Nyquist plots obtained from the CR 2032-coin cell battery, both with and without UV light irradiation. The highest frequency region of a Nyquist plot provides information about the electrical resistance of the electrolyte solution (Re). The average electrical resistance of the $LiPF_6$ liquid electrolyte was approximately 2Ω. While the middle-frequency region provides information on the charge transfer that occurs at the $LiMn_2O_4$/ $LiPF_6$ electrolyte interface.

The coin cell battery that was not exposed to UV irradiation exhibited a charge transfer resistance of 8056 Ω at the $LiMn_2O_4$/ $LiPF_6$ electrolyte interface. This value is higher than the charge transfer resistance measured under UV light irradiation, which was 7940 Ω. The observed reduction in charge transfer resistance at the $LiMn_2O_4$/ $LiPF_6$ electrolyte interface indicates that UV light irradiation lowers the resistance and accelerates the movement of lithium ions across the interface, resulting in more efficient electron transfer.

The observed result can be illustrated in the schematic of Fig 8(b). In general, the application of UV light irradiation causes electrons to jump from the valence band to the conduction band of $LiMn_2O_4$, leading to the generation of electron-hole pairs. The formation of these charge carriers at the $LiMn_2O_4$, surface enhances charge transfer at the electrode/electrolyte interface. This improved process enables the CR 2032-coin cell battery to achieve a shorter charging time (Fig 7).

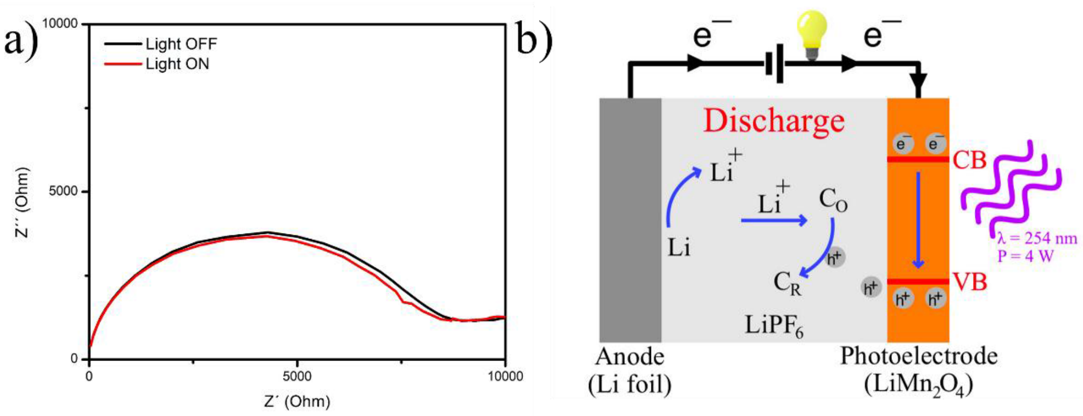

Fig 8. (a) Comparison of the Nyquist plot of a CR2032 coin cell battery without UV light irradiation and with UV light irradiation and (b) a schematic representation of the photoactive process in batteries. Figure is designed based on the models presented in Refs [23] and [24].

4 Conclusion

This communication reports on the fabrication of a $LiMn_2O_4$ coin cell battery equipped with a transparent window. It also investigates the effect of UV light irradiation on the electrochemical performance of the $LiMn_2O_4$ coin cell battery. The study concluded that UV light irradiation at a low power of 4W provides sufficient energy to induce photoactivity in the $LiMn_2O_4$ cathode material. Specifically, this energy allows electrons to jump from the valence band to the conduction band of the $LiMn_2O_4$, generating electron-hole pairs at the cathode surface. The generation of these charged particles reduces the electronic resistance of charge transfer at the $LiMn_2O_4$ / $LiPF_6$ electrolyte interface. This improvement facilitates a more efficient movement of lithium ions across the interface, resulting in a shorter charging time, with voltages increasing from the open-circuit voltage (OCV) state to a charging state of 4.2V.

This work contributed to the development of novel technologies that utilize photoactive processes in lithium batteries, presenting a promising avenue to accelerate charging in the transition to sustainable energy.

Acknowledgements

The research described in this publication was made possible in part by:

Consejo Nacional de Humanidades, Ciencia y Tecnología from México (CONAHCYT) for the financial support grant CBF2023-2024-3089 "*Novedosa caracterización espectroscópica para baterías: Análisis de la estructura de bandas en microbaterías de película delgada de estado sólido en operación (carga- descarga) mediante Espectroscopia Fotoelectrónica de rayos X* (*XPS*)".

El Ministerio de Relaciones Internacionales y de la Francofonia (MRIF) de Quebec, la Delegación General de Quebec en México (DGQM) y AMEXCID for the financial support grant OPM/00182/2024 "*Investigaciones Raman in situ para mejorar la resistencia a la fatiga de sistemas de almacenamiento de energía de iones de litio*".

Instituto de Innovación Ciencia y emprendimiento para la competitividad (INNOVACION) for the financial support grant SOL-2052 (Estudios de Espectroscopia Raman In Situ para Mitigar la Fatiga en baterías de Iones de Litio)

The authors thank Christian Albor Cortes for her technical support on SEM measurements.

References

1. IRENA (2024), World Energy Transitions Outlook 2024: 1.5°C Pathway, International Renewable Energy Agency, Abu Dhabi. https://www.irena.org/-/media/Files/IRENA/Agency/Publication/2024/Nov/IRENA_World_energy_transitions_outlook_2024.pdf.
2. Nitta N, Wu F, Lee J T, Yushin G, Li-ion battery materials: present and future, *Materials Today*, 18(2015)252–264.
3. Whittingham M S, Lithium batteries and cathode materials, *Chem Rev*, 114(2014)11414–11443.
4. Manthiram A, An outlook on lithium ion battery technology, *Nature Commun*, 8(2017)15103; doi.org/10.1021/acscentsci.7b00288.
5. Julien C M, Massot M, C Poinsignon, Lattice vibrations of manganese oxides: Part I. Periodic structures, *Mater Sci Eng B*, 97(2003)217–230.
6. Ambriz-Vargas F, Garza-Hernández R, Martínez-Flores S, Aguirre-Tostado F S, Martínez-Guerra E, Quevedo-López M, Fine-Tuning Cathode Performance: The Influence of Argon Deposition Pressure on $LiMn_2O_4$ Thin Film Electrochemistry for Li-Ion Batteries, *Batteries*, 449(2024); doi.org/10.3390/batteries10120449.
7. Dixit M, Srivastava S, Jain A, A comprehensive review of fast charging infrastructure for electric vehicles: Perspectives, standards, and developments, *J Energy Storage*, 35(2021)102255; doi:10.1080/23080477.2018.1437323.
8. Thackeray M M, David W I F, Bruce P G, Goodenough J B, Lithium insertion into manganese spinels, *Mater Res Bull*, 18(1983)461–472.
9. Manthiram A, Yu X, Wang S, Lithium battery chemistries enabled by solid-state electrolytes, *Nat Rev Mater*, 2 (2017)16103; doi.org/10.1038/natrevmats.2016.103.
10. Lee A, Vörös M, Dose W M, Niklas J, Poluektov O, Schaller R D, Iddir H, Maroni V A, Lee E, Ingram B, Curtiss L A, Johnson C S, Photo-accelerated fast charging of lithium-ion batteries, *Nat Commun*, 10(2019)4946; doi.org/10.1038/s41467-019-12863-6.
11. Hee-Je K, Krishna T N V, Zeb K, Rajangam V, Chandu V V, Gopi M, Sambasivam S, Raghavendra K V G, Obaidat I M, A Comprehensive Review of Li-Ion Battery Materials and their Recycling Techniques, *Electronics*, 9 (2020), 1161; doi.org/10.3390/electronics9071161.
12. Ortiz Y, Arévalo P, Peña D, Jurado F, Recent Advances in Thermal Management Strategies for Lithium-Ion Batteries: A Comprehensive Review, *Batteries*, 10(2024)83; doi.org/10.3390/batteries10080265.
13. Zhang S, Deng W, Momen R, Yin S, Chen J, Massoudi A, Zou G, Hou H, Deng W, Ji X, Element substitution of a spinel $LiMn_2O_4$ cathode, *J Mater Chem A*, 9(2021)21532–21550.
14. Berg H, Thomas J O, Neutron diffraction study of electrochemically delithiated $LiMn_2O_4$ spinel, *Solid State Ion*, 123(1999)227–234.
15. Tang D, Sun Y, Yang Z, Ben L, Gu L, Xuejie H, Surface Structure Evolution of $LiMn_2O_4$ Cathode Material upon Charge/Discharge, *Chem Mater*, 26(2014)3535–3543.
16. Nishimura K, Douzono T, Kasai M, Andou H, Muranaka Y, Kozono Y, Spinel-type lithium–manganese oxide cathodes for rechargeable lithium batteries, *J Power Sources*, 81–82(1999)420–424.
17. Douafer S, Lahmar H, Benamira M, Rekhila G, Trari M, Physical and photoelectrochemical properties of the spinel $LiMn_2O_4$ and its application in photocatalysis, *J Phys Chem Solids*, 118(2018)62–67.
18. Tan R, Hwang S W, Sivanantham A, Cho I S, Solution synthesis and activation of spinel $CuAl_2O_4$ film for solar water-splitting, *J Catal*, 400(2021)218–227.
19. Kirankumar V S, Sumathi S, A review on photodegradation of organic pollutants using spinel oxide, *Mater Today Chem*, 18(2020)100355; doi.org/10.1016/j.mtchem.2020.100355
20. Radzi Z, Arifin K, Kufian M, Balakrishnan V, Raihan S, Rahim N, Subramaniam S, Review of spinel $LiMn_2O_4$ cathode materials under high cut-off voltage in lithium-ion batteries: Challenges and strategies, *J Electroanal Chem*, 920(2022)116623; doi.org/10.1016/j.jelechem.2022.116623.
21. Kim S, Kumar V, Seo D, Park Y, Kim J, Kim H, Kim J, Hong J, Kang K, Invited Paper: Preparation and Electrochemical Characterization of Doped Spinel $LiMn_{1.88}Ge_{0.1}Li_{0.02}O_4$ Cathode Material, *Electron Mater Lett*, 7(2011)105–108.

22. Guan-Jhu C, Wei-Hsin C, Evaluation of Charging Methods for Lithium-Ion Batteries, *Electronics*, 12(2023)4095; doi.org/10.3390/electronics12194095.
23. Shimokawa K, Matsubara S, Okamoto A, Ichitsubo T, Light-induced Li extraction from $LiMn_2O_4/TiO_2$ in a water-in-salt electrolyte for photo-rechargeable batteries, *Chem Commun*, 58(2022)9634–9637.
24. Zhang P, Cai M, Wei Y, Zhang J, Li K, Silva S R P, Shao G, Zhang P, Photo-Assisted Rechargeable Metal Batteries: Principles, Progress, and Perspectives, *Adv Sci*, 30(2024)2402448; doi.org/10.1002/advs.202402448.

[*Received*: 17.12.2024; *rev recd*: 29.12.2024; *accepted*: 30.12.2024]

David Alejandro Medina Sánchez obtained his Master of Science degree from the University of Guanajuato in 2012. In September 2022, he enrolled in the Optics doctorate program at the Centro de Investigaciones en Óptica, where his research focuses on studying the interaction of light with internal battery components.

Email: davidms@cio.mx

Jose Salvador Martinez Flores earned his Master of Science degree from the Center for Research and Advanced Studies (CINVESTAV) in 2022. He is currently workig as the laboratory technician for the clean room facilities at the Centro de Investigaciones en Óptica.

Email: smartinez@cio.mx

Salomon Rodriguez Carrera earned his Master of Science degree from the Centro de Investigaciones en Óptica in 2011. In September 2023, he enrolled in the Interinstitutional Doctorate Program at the same center, where his research focuses on the fabrication and evaluation of fuel cells.

Email: salomonrc@cio.mx

Luis Salvador Valle Garcia earned his Master of Science degree from the University of Guanajuato in 2018. In September 2024, he enrolled in the Interinstitutional Doctorate program at the Centro de Investigaciones en Óptica, where his research focuses on the synthesis of solid-state electrolytes for the fabrication of GEN 4 energy storage devices.

Email: lsvalle@cio.mx

Cesia Daniela Mena Muñoz is currently a Master of Science student at the Centro de Investigaciones en Óptica, where her research work focuses on the development of silicon anodes with high specific capacity.

Email: danielamm@cio.mx

Lilian Skokan earned her Master of Science degree from the Institut National de la Recherche Scientifique in 2022. She is currently enrolled in the Ph D program at the same institute, where her research focuses on the study of materials using Raman spectrometry.

Email: Lilian.Skokan@inrs.ca

Sebastian Obernberger earned his Master of Science degree from Hochschule München University of Applied Sciences in 2022. He is currently enrolled in the Ph.D. program at the Institut National de la Recherche Scientifique, where his research focuses on developing semiconductor materials for electronic devices.

Email: sebastian.obernberger@inrs.ca

Andreas Rüdiger obtained his bachelor's degree in Physics in 1997 at the University of Osnabrück, Germany. In 2001, he completed his Ph D in Physics, focusing on electron paramagnetic resonance studies in ferroelectric materials. Currently, Andreas Rüdiger is a Professor at the Énergie Matériaux Télécommunications Research Center, located in Varennes, Quebec, Canada, and works as an ambassador for the German Academic Exchange Service.

Email: Andreas.Ruediger@inrs.ca

Raquel Hernandez Garza earned her doctorate from the Centro de Investigación en Materiales Avanzados (CIMAV) in 2019. She then worked as a postdoctoral researcher at the University of Illinois in 2023. Currently, she is a research engineer at the Centro de Investigaciones en Óptica, where her work focuses on the development of novel materials for sodium energy storage devices.

Email: rgarza@cio.mx

Francisco Morales Morales earned his doctorate from the Benemérita Universidad Autónoma de Puebla (BUAP). He then worked as a postdoctoral researcher at the Centro de Investigación en Materiales Avanzados (CIMAV) for two years, from 2018 to 2019. Currently, he serves as a research engineer at the Centro de Investigaciones en Óptica, where he focuses on developing novel silicon anode materials.

Email: fcomm@cio.mx

Alfredo Benitez Morales received his doctorate from the Benemérita Universidad Autónoma de Puebla (BUAP). He subsequently worked as a postdoctoral researcher at the University of Texas. Currently, he is a researcher at the National Institute of Astrophysics, Optics, and Electronics, where he focuses on developing innovative silicon anode materials.

Email: alfredom@inaoep.mx

Fabian Ambriz Vargas received his Ph D from the Institut National de la Recherche Scientifique in 2018. He then spent two years as a postdoctoral researcher at the Thermal Plasma Laboratory at Concordia University. Currently, he works as a researcher in energy storage at the Centro de Investigaciones en Óptica, focusing on the development of novel materials for lithium energy storage devices.

EMAIL: fambriz@gmail.com